AD-A089 730 ROCKWELL INTERNATIONAL THOUSAND OAKS CA SCIENCE CENTER F/G 20/4
WAVE INTERACTIONS IN TRANSONIC AND HYPERSONIC FLOW.(U)
AUG 80 N D MALMUTH F44620-76-C-0044
UNCLASSIFIED SC5054.5FR AFOSR-TR-80-0752 NL

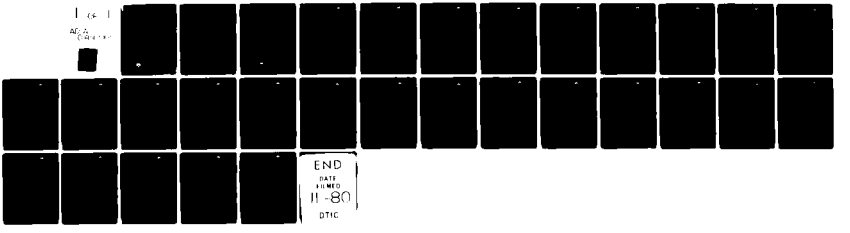

END
DATE FILMED
11-80
DTIC

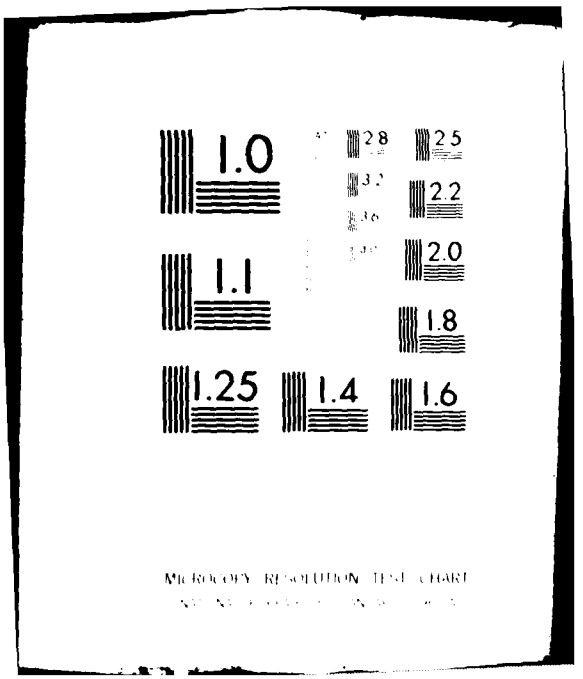
1.0
1.1
1.25
1.4
1.6
2.0
2.2
2.5
MICROCOPY RESOLUTION TEST CHART

SC5054.5FR

WAVE INTERACTIONS IN TRANSONIC AND HYPERSONIC FLOW

FINAL TECHNICAL REPORT FOR THE PERIOD 1 December 1975 through 31 May 1980

CONTRACT NO. F44620-76-C-0044
PROJECT NO. 2307

Prepared for

Air Force Office of Scientific Research

By

Dr. N. D. Malmuth
Principal Investigator

AUGUST 1980

This research was sponsored by the Air Force Office of Scientific Research (AFSC), United States Air Force, under Contract F44620-76-C-0044

Rockwell International,
Science Center,
Thousand Oaks, Ca.

(14) SC5054.5FR

(6) WAVE INTERACTIONS IN TRANSONIC AND HYPERSONIC FLOW

(9) Final Technical Report for the Period
1 Dec 1975 through 31 May 1980

(15) Contract No. F44620-76-C-0044
Project No. 2307
(16)

Prepared for

Air Force Office of Scientific Research

By

(10) Dr. N.D. Malmuth
Principal Investigator

(11) August 1980 (12) 34

(18) AFOSR

This research was sponsored by the Air Force Office of Scientific Research (AFSC), United States Air Force, under Contract F44620-76-C-0044

(19) TR-80-0752

Rockwell International
Science Center

CONTENTS :

ILLUSTRATIONS

FINAL TECHNICAL REPORT FOR AFOSR CONTRACT F44620-76-C-0044,
PROJECT NO. 2307, FOR THE PERIOD
1 DECEMBER 1975 THROUGH 31 MAY 1980

Comprehensive List of Research Objectives

a. Study hypersonic and transonic theory with emphasis on wing-body interference and other nonplanar problems.

b. Study refraction, reflection and diffraction processes occurring in nonlinear wave propagation in steady and unsteady flows.

c. Investigate transonic wind tunnel wall interference in steady and unsteady flows.

d. Apply inverse solvers to slender configurations in transonic flow.

Substantive Statement of Significant Accomplishments and Progress Toward Achieving Research Objectives

Regarding Items a and b, new analytical hypersonic flow solutions over glide vehicles consisting of delta wing-bodies were obtained giving insight into the important role of such geometric features as the longitudinal area progression of the body. A generalized area rule was developed in which the change in L/D of the clean delta wing due to body addition could be quantified solely in terms of this progression and the body cross-sectional shape. Details of this rule are given in C3 in the Cumulative Chronological List of Publications provided in what follows. Further information with emphasis on Item b will be presented in C8. These publications deal with the nonlinear wave interaction processes occurring in hypersonic wing-body interference. Their exploitation to achieve favorable L/D and use of transparent analytical relationships derived in this contract is described in C3.

In what follows, progress related to Items c and d will be detailed.

Steady Transonic Tunnel Wall Interactions and Far Fields

A Green's function method has been developed to predict the asymptotic flow upstream and downstream of airfoils and wings in wind tunnels. Originally, the method was developed in a Karman-Guderley (KG) framework and in more recent phases has been extended to handle modified small disturbance theory (MSD) flows. The analytical results of these studies have been reported in C4 and C6, and further details and numerical results will be given in C9 and C10, as well as other publications.

As compared to the KG formulation, the effect of the MSD modifications was demonstrated to substantially change the structure of the volume source term appearing as the dominant term in the far field for the perturbation velocity potential. Additional contributions were demonstrated to occur due to the influence of vorticity on the wing and wake and sources over the wing. Analysis of the appropriate mathematical representations for these effects gave rise to the following findings:

1. For closed trailing edge wings the pressure associated with the wing confined between solid and free-jet walls damps exponentially far upstream and downstream of the wing.

2. For open trailing edges such as those associated with jet flap implementations or intermediate inverse (design) solutions, a source term evolves with solid walls which is proportional to the integral of the trailing edge thickness over the wing span and inversely proportional to the Glauert compressibility factor.

3. As in incompressible flow, for large distances downstream, the effect of the shed trailing vortices has been shown to be identical to that produced by a collection of two-dimensional vortices of individual intensity proportional to the rate of

change of the spanwise load distribution. The location of each of the two-dimensional vortices is on the projection of the corresponding trailing vortex in the Trefftz plane. For rectangular tunnel cross-sections, the appropriate expression for the induction is a double Fourier series in the transverse coordinates normalized by the characteristic height and breadth of the tunnel dimensions. This can be also expressed in terms of elliptic theta functions. The effect of the transonic nonlinearity is exhibited in the higher order terms and the near field coupling with spanwise loading. This validation of the transonic application of Biot Savart's law can be used to readily estimate the asymptotic upstream and downstream behavior associated with tunnel cross sectional shapes other than rectangular for free-jet, slotted, and solid wall boundaries. This can be achieved through the use of mapping and image reflection principles. For porous walls the procedure reverts back to the Green's theorem method. Here, an unconventional Sturm Liouville problem arises in which the eigenvalues appear in the boundary conditions.

4. For closed trailing edges, the exponential damping exhibited by the tunnel-wall far field solution contrasts with the algebraic behavior associated with the free-field configuration. For open trailing edges, the associated source effect damps algebraically with distance in contrast to the growth behavior exhibited for the confined wall case indicated in (2).

More recent phases of the effort deal with assessment of tunnel wall interference on compound lifting units. Typical results from C7 are shown in Fig. 1. These show the effects of solid walls on the mutual aerodynamic interaction between dual lifting elements representative of

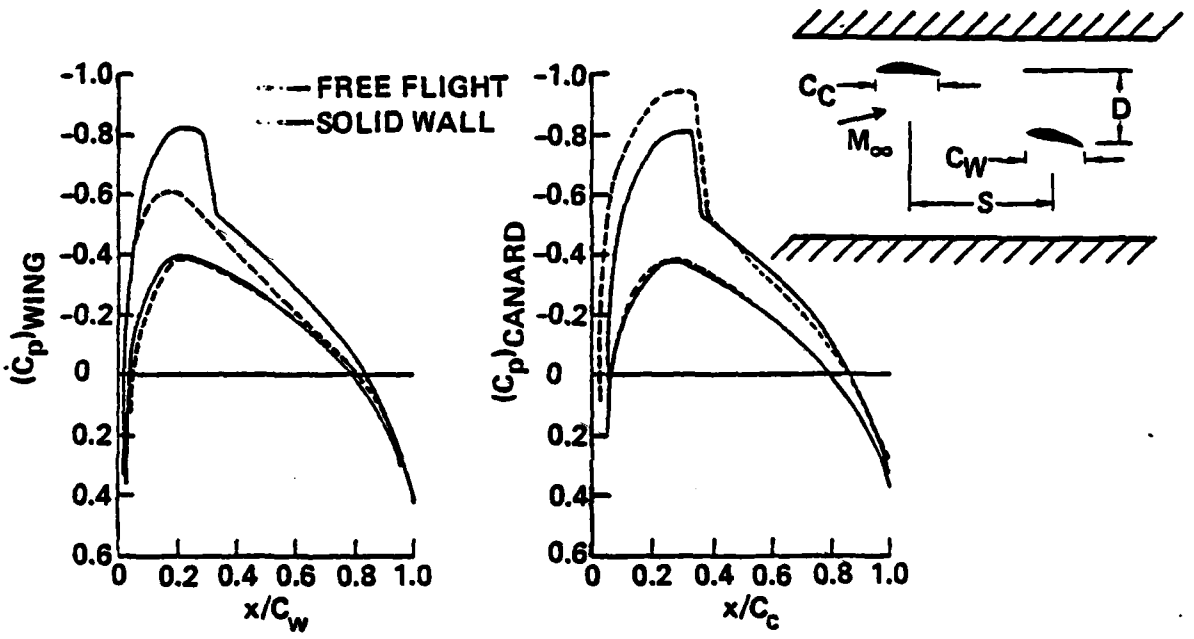

Fig. 1. Comparison of free flight and solid tunnel wall, pressure distributions for 2-D canard-wing system. $M_\infty = 0.75$, $\alpha_W = \alpha_C = 1°$, $H/C_W = 3.75$, $S = -2$, $C_W = 2$, $C_C = 1.2$, $D = 2$.

a two-dimensional characterization of canard-wing interference. These calculations used special far fields developed for multiple systems. The chordwise pressure distributions indicate that the wall choking effect increases the rear lifting surface (wing) effective incidence angle, apparently resulting in a larger supercritical region and the addition of a terminating shock. On the other hand, the forward lifting surface (canard) experiences a lower incidence angle compared with the free flight case, and the shock is much weaker. These striking trends could reverse with other combinations of the parameters such as gap, stagger, Mach number and incidence but are felt indicative of variations of an important subclass of these variables. Additional far field analytical results which apply to slotted and free jet cases are described in C7 with a summary of the analysis. Details will be given in C9 and C10. Some of these results have been presented at the recent Adaptive Wall Symposium at AEDC in I7 and relate to important difficulties in accounting for multi-wing interactions in the convergence of the adaptive wall iteration process in obtaining interference free results for the tail chordwise pressures.

A special phase of the research effort has been devoted to the nonself-adjoint problems associated with modeling porous walls. These studies which will be reported in C10 are being used to assess blockage effects and can be generalized to the treatment of adaptive tunnels. Because of a difficulty associated with an eigenvalue appearing in the boundary conditions for the porous case, special procedures were developed in FY 1979 to determine the Green's function which appears as a kernel in the integral representation for the perturbation potential and is a solution to the nonself-adjoint boundary value problem. Our new method utilizes auxiliary functions which form a "dual basis" of eigenfunctions having self-adjoint properties and orthogonality. With this procedure, the Green's function has been developed for circular test sections as

an example of the approach which has been conceptualized for arbitrary cross sections. This work will serve as a basis for the continuation of the effort dealing with a systematic asymptotic procedure for the assessment of tunnel wall blockage effects, *expanding the focus to near field aspects* in addition to the downstream and upstream behavior currently being investigated.

Another portion of the effort has involved sensitivity analyses regarding the near field impact of errors in the satisfaction of the correct far field boundary conditions in a wind tunnel environment. This activity is partially motivated by adaptive wall applications. For the linear case, a perturbation formulation has been used to show that an error in the estimate of the far field produces the same order of effect in the near field. For the nonlinear case, this generalization is not immediately evident, and numerical methods are currently being utilized to provide information regarding the effects of such parameters as wall height, chord and control section lengths.

Typical results from these two-dimensional studies are shown in Figs. 2-4. For these calculations, a NACA 0012 was modeled in a solid wall tunnel using a two-dimensional SLOR solver for the Karman-Guderley transonic small disturbance model. The far field was computed using expressions from C7. In Fig. 4, confined lift coefficients are plotted as a function of the streamwise location of the upstream and downstream control boundaries situated at x_F chord lengths from the center of the airfoil which is situated on the tunnel centerline. The calculations, which were performed at $M_\infty = 0.75$ and $\alpha = 2°$, retaining only the dominant terms in the far field indicate that the appropriate $x_F = \infty$ asymptotic value is approached more rapidly for lower height to chord ratios, H. This trend is symptomatic of the transition of decay of disturbances between small and large H. For smaller values of this parameter, our

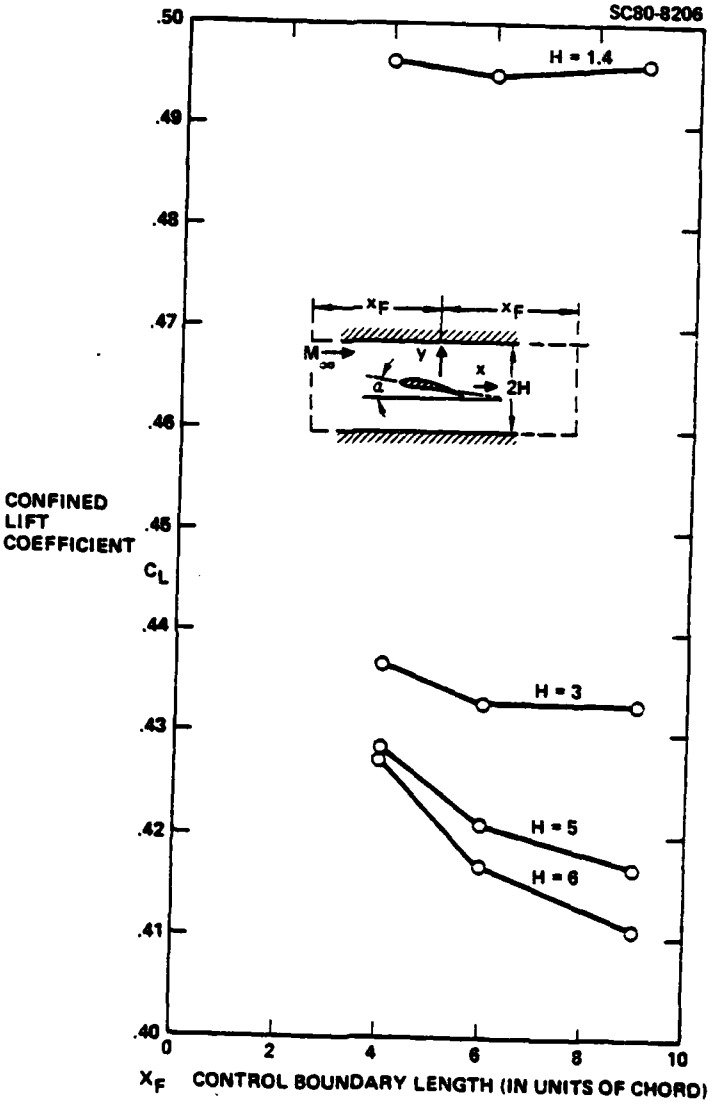

Fig. 2. Convergence of C_L's to $x_F = \infty$ value in solid wall tunnel, $M_\infty = 0.75$, $\alpha = 2°$, NACA 0012 airfoil, only dominant far field terms used.

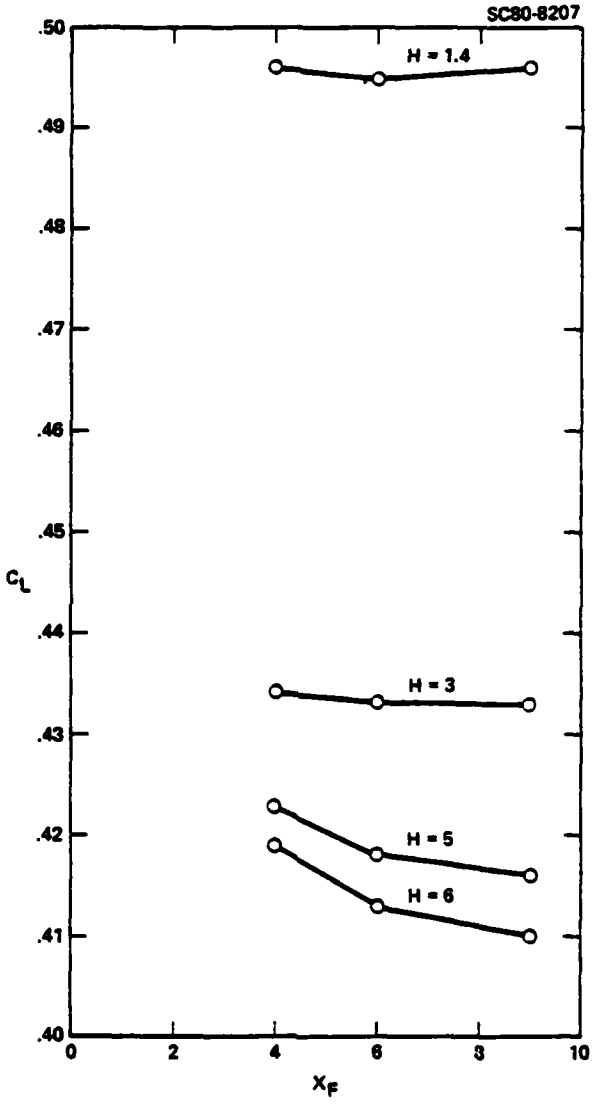

Fig. 3. Convergence of C_L's to $x_F = \infty$ value in solid wall tunnel, $M_\infty = 0.75$, $\alpha = 2°$, NACA 0012 airfoil, far field expansion taken to second order.

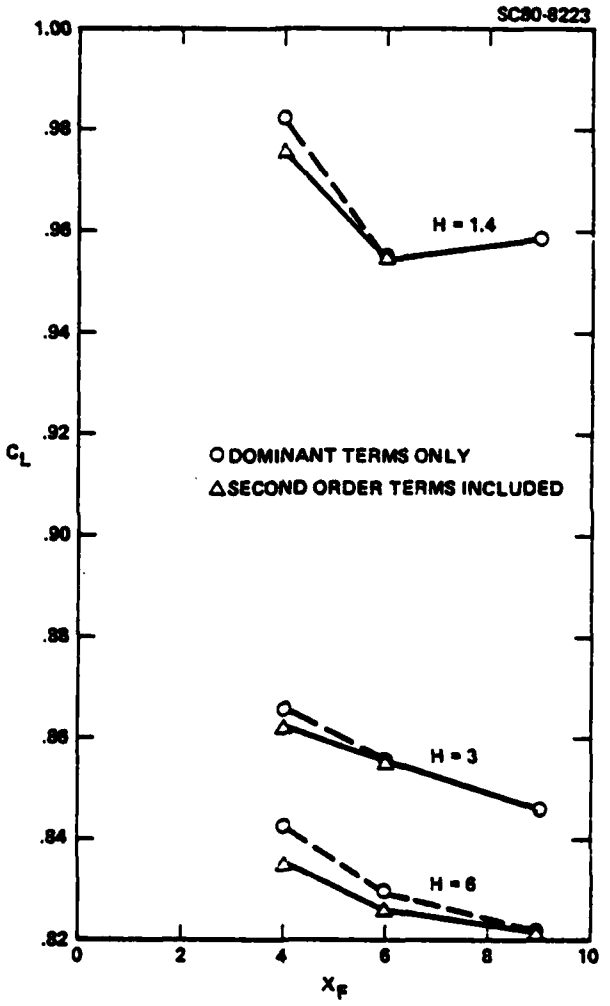

Fig. 4. Convergence of C_L's to $x_F = \infty$ value in solid wall wind tunnel, $M_\infty = 0.75$, $\alpha = 4°$, NACA 0012 airfoil, comparison of retention of various terms in far field.

far field research has indicated that the decay is exponential, whereas for large values it becomes algebraic, appropriate to the free field. This behavior will be a crucial part of the matching aspects in the asymptotic tunnel interference theory.

In Fig. 3, similar studies were performed indicating the approach to the asymptotic values of the confined lift coefficients with a second order expression for the far field. Here, it is evident that inclusion of more terms speeds up the approach to the asymptotic C_L. Accordingly, the dimensions of the computational domain can be reduced. For adaptive walls, the significance of this result is to reduce the streamwise extent of the control domain. Figure 4 reaffirms these trends at $\alpha = 4°$ and also indicates the larger x_F required to reach the asymptotic values. This trend is associated with the stronger disturbances produced by the larger incidence.

To study analogous trends in three-dimensional flows, parametric studies were performed using the geometry indicated in Fig. 5. Here, a rectangular planform wing with a NACA 65A006 section was simulated in a rectangular cross section solid wall tunnel. Calculations were performed for varying M_∞, α, H, D, and wing aspect ratio, studying the decay of the pressure field with x_F in this investigation. For the geometry considered, the far field analytic formula further developed in recent phases of the current contract can be written in the form (using the notation of Fig. 5)

$$\phi = \phi_{FF} = I_W + I_{wa} + I_T + I_{VS} \quad \text{as} \quad x \to \pm\infty \tag{1a}$$

where

$$I_W = \frac{e^{-\lambda|x|}}{\pi D} \sin \lambda y \int_0^B d\zeta \int_{x_{LE}K^{-1/2}}^{x_{TE}K^{-1/2}} e^{\lambda\xi}[u]d\xi \quad , \quad u \equiv \phi_x \tag{1b}$$

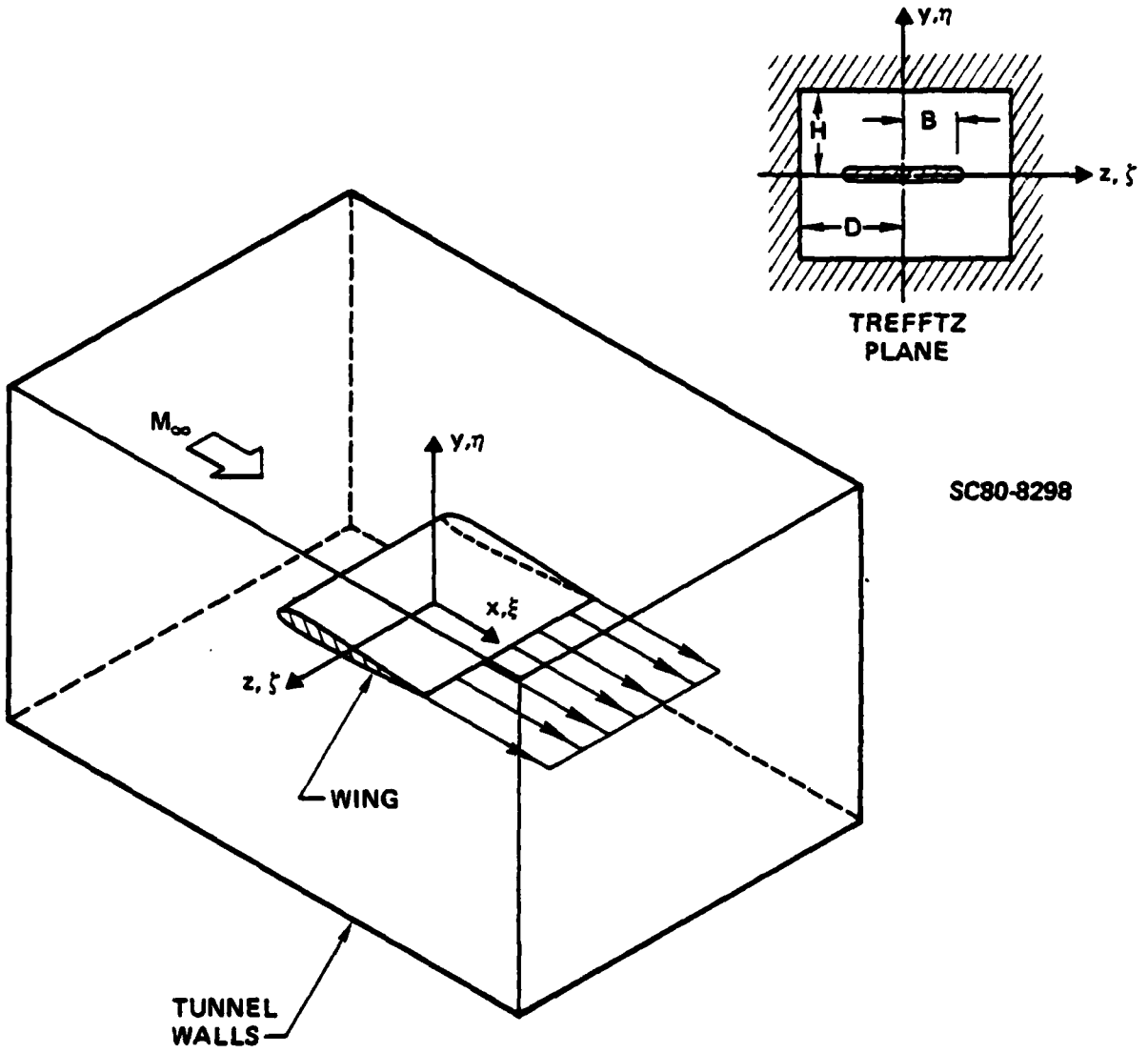

Fig. 5. Rectangular wing in rectangular cross section tunnel.

$$I_{wa} = -\frac{2H(x)}{HD}\sum_{n=0}^{\infty}\sum_{m=0}^{\infty}\left\{\frac{\epsilon_{nm}}{\omega_{nm}^2}\left[\frac{1-(-1)^n}{2}\right](-1)^{\frac{n+1}{2}}\frac{\pi n}{2H}\right\}$$

$$\times\left\{(-1)^{\frac{m}{2}}\cos\frac{n\pi(y+W)}{2H}\cos\frac{m\pi(z+D)}{2H}\left[\frac{1+(-1)^m}{2}\right]\int_0^B[\phi]_{TE}\cos\frac{m\pi\zeta}{2D}\,d\zeta\right\}$$

$$\pm\frac{e^{-\lambda|x|}}{\pi D}\sin\lambda y\int_0^B e^{\pm\lambda x_{TE}}[\phi]_{TE}\,d\zeta \qquad (1c)$$

$$l_T = \frac{H(x)}{\sqrt{K}\,HD}\int_0^B d\zeta\int_{x_{LE}K^{-1/2}}^{x_{TE}K^{-1/2}} t(\xi,\zeta)d\xi \qquad (1d)$$

$$\frac{K^{3/2}I_{VS}}{\gamma+1} = \frac{H(x)}{4HD}\int_{-H}^{H}d\eta\int_0^D d\zeta\int_{-\infty}^{\infty}u^2d\xi$$

$$-\frac{1}{2HD}e^{-\lambda|x|}\sin\lambda y\int_0^D d\zeta\int_{-H}^{H}\sin\lambda\eta\,d\eta\int_{-\infty}^{\infty}e^{\pm\lambda\xi}u^2d\xi \qquad (1e)$$

$\lambda = \omega_{On} = \frac{\pi}{2H}$

LE ∿ Leading Edge

TE ∿ Trailing Edge

H(x) = Heaviside function

$$\omega_{mn}^2 = \left(\frac{\pi n}{2H}\right)^2 + \left(\frac{\pi m}{2D}\right)^2$$

$$\varepsilon_{mn}^{-1} = (1 + \delta_{n0})(1 + \delta_{0m}) \quad , \quad n + m \neq 0$$

δ_{nm} = Kronecker delta function .

Equations (11) can be summarized in the form:

$$\phi_{FF} \doteq A(y,z)H(x) + Be^{-\lambda|x|} \sin \lambda y \quad \text{as} \quad |x| \to \infty \tag{2}$$

where A and B can be obtained by comparison with (11).

Some typical results of the parametric studies will now be discussed. In Fig. 6, calculations for the downstream decay of the absolute value of pressure on the bottom wall $|\phi_x(x,-H,0)|$ are shown with a simplified version of (12), $\phi_x(x,y,\pm 20c) = 0$, imposed at the computational upstream and downstream boundaries. For the cases to be discussed hereinafter, $M_\infty = 0.9$ and $\alpha = 5°$. The correct decay rate as shown by the dash dot line from (12) is compared to the numerically obtained result, indicating that placing the infinity boundary condition at a finite upstream and downstream location still produces exponential decay but with a decay rate different than λ.

Figure 7 indicates the effect of utilizing the two term asymptotic Eqs. (1) in the far field. For an intermediate range of x, it is evident from the plot that the wall pressure distribution correctly tracks the proper decay rate for x_F sufficiently large, i.e., 20. The lack of correlation near the wing is expected since that region is nonlinear. This behavior gives an indication of the control length limits for adaptive wall applications. It is furthermore significant that anamolous results

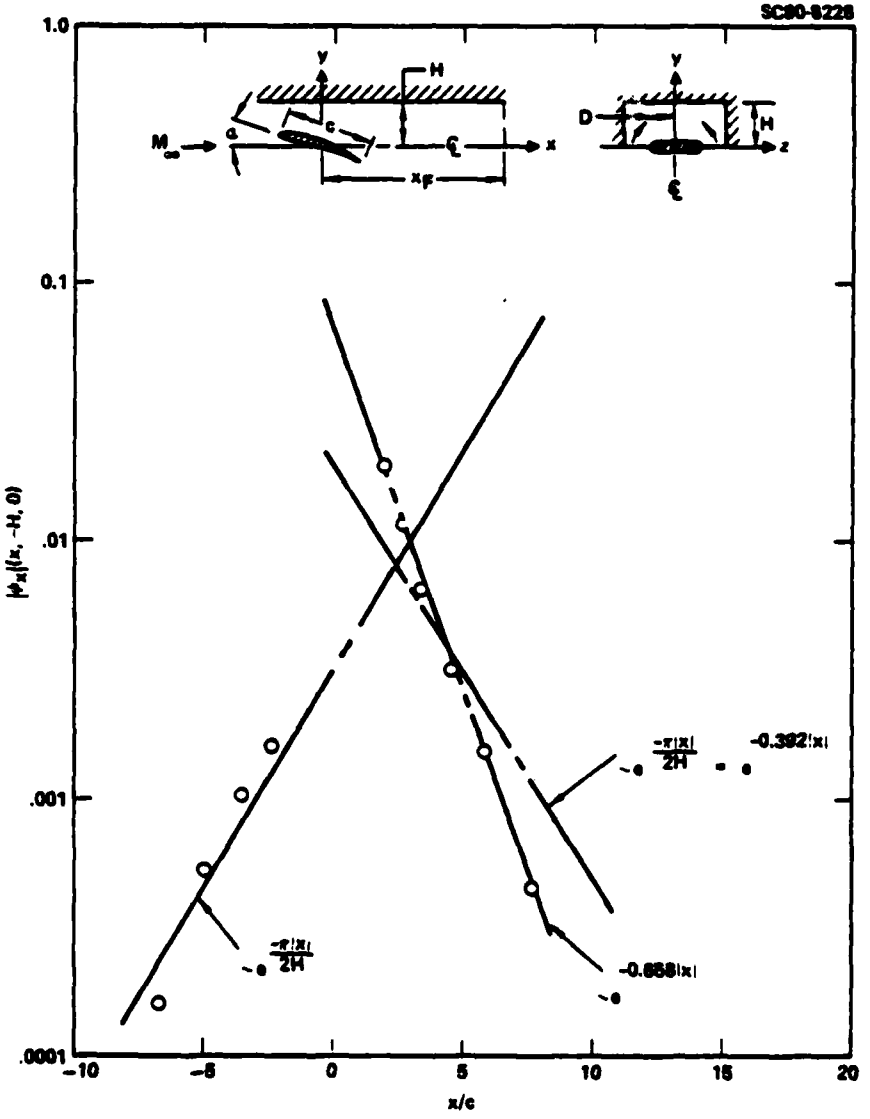

Fig. 6. Upstream and downstream decay of absolute value of pressure, H = D = 4c, M_∞ = 0.9, α = 5°, NACA 65A006 section, AR = 2, $\phi_x(x,y,\pm 20c) = 0$.

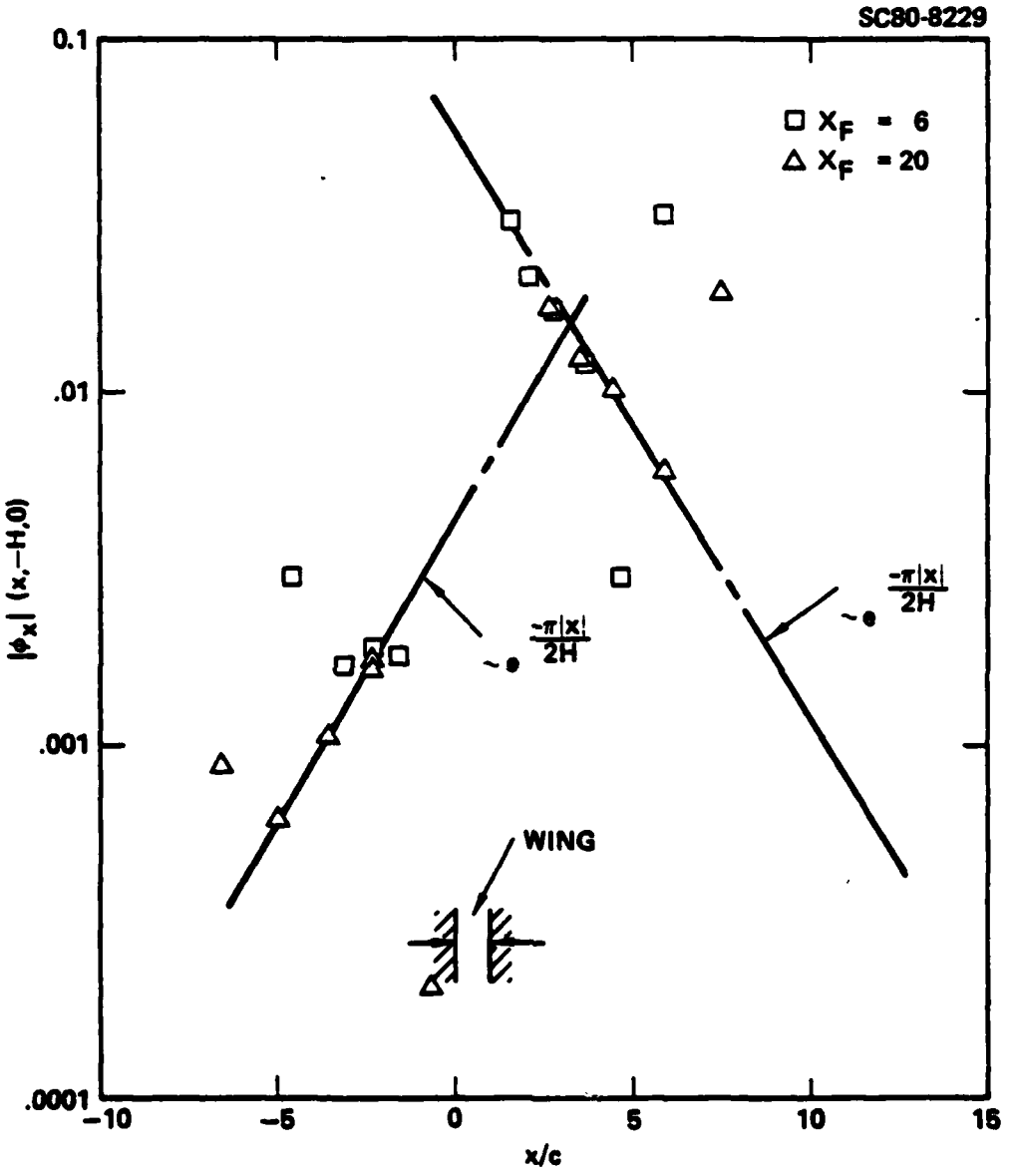

Fig. 7. Upstream and downstream decay of absolute value of pressure, H = D = 4c, M_∞ = 0.9, α = 5°, NACA 65A006 section, AR = 2, far field given by Eqs. (1).

are obtained for x large where a new phenomenon takes place. Here, discretization errors resulting from the expanded grid overshadow the alleged improved accuracy of the Prandtl-Glauert asymptotic (1). A more correct picture than that obtained from the analytical far field analysis leading to (1) would evolve from a study of the relevant difference equation properties rather than the continuum limit as $x \to \infty$. This limit is extremely subtle involving a combination of the expanding mesh and large x. As for the continuum formulation, the discrete problem is linear. Appropriate solution procedures are currently under study.

In Figs. 8 and 9, the significance of the far field in regard to the value of the lift and drag coefficient on the rectangular wing for the previous values of the parameters is shown. Here, the free field coefficient is denoted on the ordinate scale by the indicated arrows. From these results, it is obvious that the position of the control boundary has a decisive effect on the magnitude of the force coefficients. Studies such as these give rise to the striking conclusion that the location of the far field downstream control boundary can affect the lift coefficient by an amount exceeding the basic solid wall blockage correction to the free field values. This emphasizes the significance of the proper application of downstream and upstream far field conditions in adaptive and nonadaptive tunnel interference modeling.

Unsteady Tunnel Wall Interference Effects

For unsteady wind tunnel flows, a mathematical framework schematically indicated in Figs. 10 and 11 has been devised to provide a consistent approximation procedure for the characterization of the far fields. This approach corresponds to the unsteady counterpart of the integral representation method utilized for steady confined flows. Results obtained

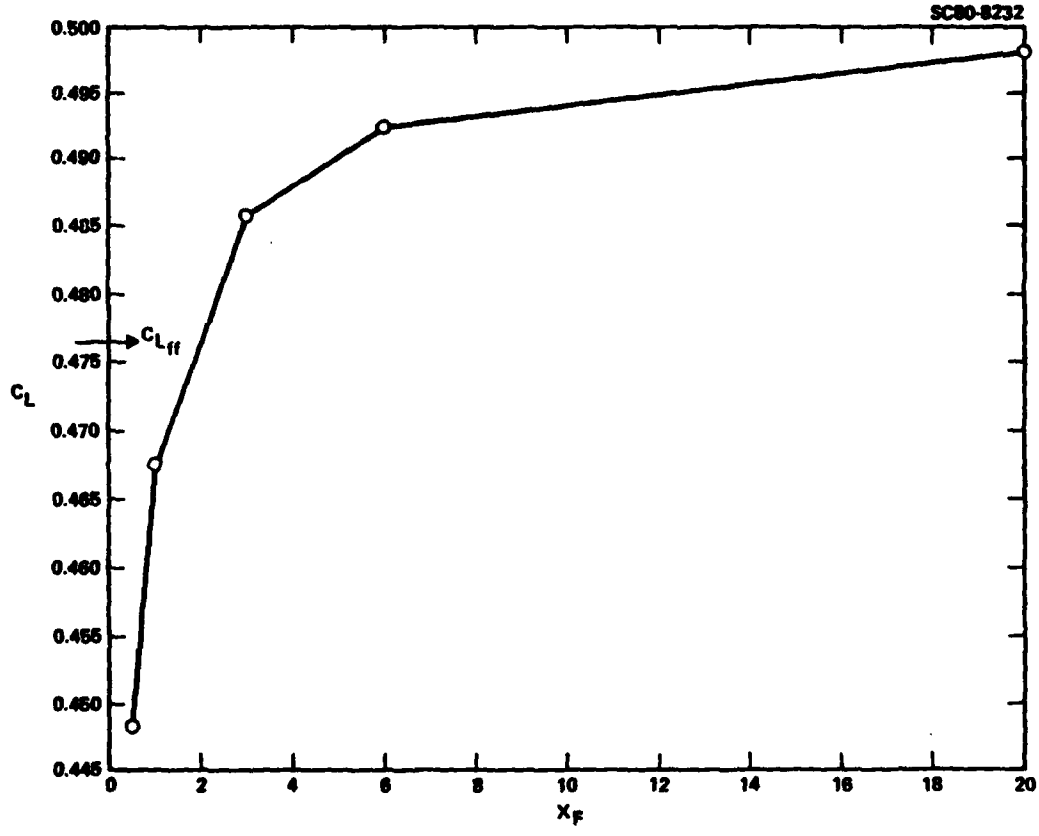

Fig. 8. Sensitivity of C_L to x_F, $M_\infty = 0.9$, $\alpha = 5°$, $H = D = 4c$.

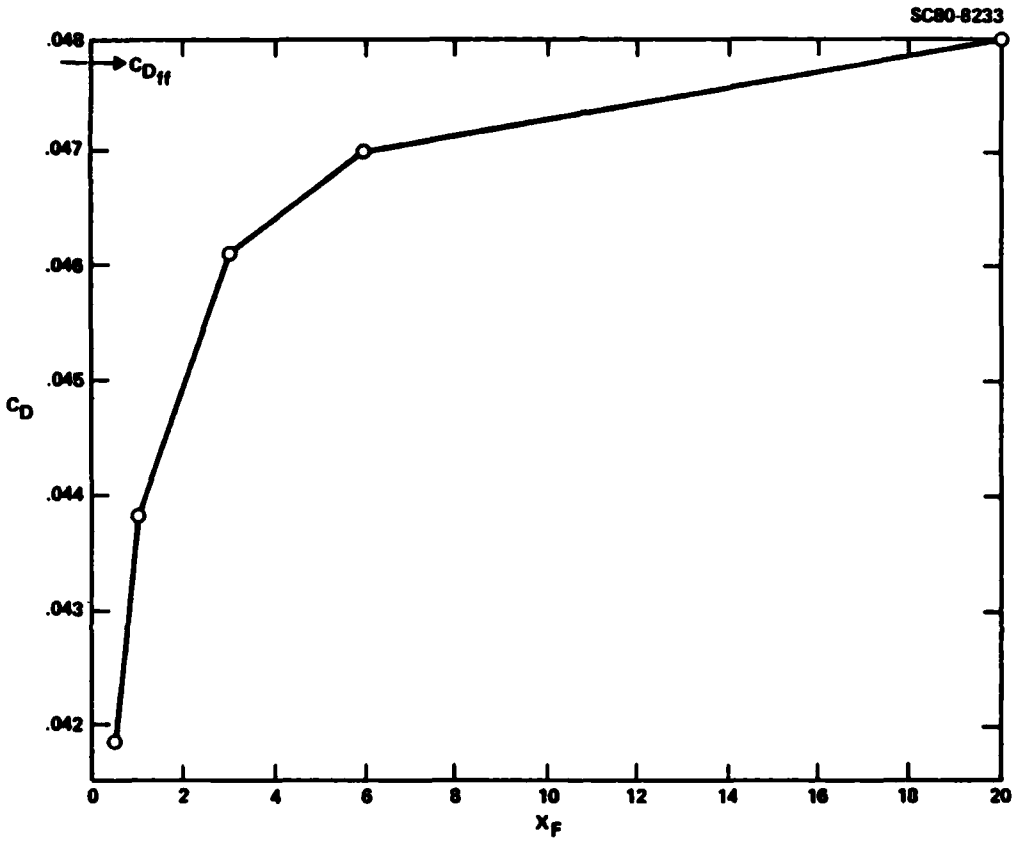

Fig. 9. Sensitivity of C_D to x_F, $M_\infty = 0.9$, $\alpha = 5°$, $H = D = 4c$.

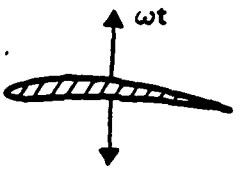

SCALE TRANSFORMATIONS

$$y^* = \sqrt{K}\,\bar{y}$$

$$\phi(x^*,y^*,t^*) = e^{i\omega t}\psi(x^*,y^*)$$

$$\psi = e^{i(\omega/K)x^*}\Lambda(x^*,y^*)$$

OUTLINE OF SOLUTION – (FREE FIELD)

BASIC TRANSFORMED EQUATION

$$\Lambda_{xx} + \Lambda_{yy} + \frac{\omega^2}{K^2}\Lambda = Q(x,y,t)$$

NONLINEAR SOURCE

EFFECTIVELY, A PARAMETER

FUNDAMENTAL HELMHOLTZ SOLUTION

$$G = \frac{i}{4} H_0^{(2)}\left(\frac{\omega r}{K}\right)$$

H_0 = HANKEL FUNCTION OF SECOND KIND

$$r = \sqrt{(x-\xi)^2 + (y-\eta)^2}$$

INTEGRAL REPRESENTATION

$$-\Lambda = \int_{-1}^{1} \langle G \rangle \left[\frac{\partial \Lambda}{\partial \eta}\right] d\xi - \iint_{-\infty}^{\infty} G(x,y;\xi,\eta) Q(\xi,\eta,t)\, d\xi d\eta$$

$$2\langle\ \rangle = (\ )_{\eta=0+} + (\ )_{\eta=0-}$$

$$[\ ] = (\ )_{\eta=0+} - (\ )_{\eta=0-}$$

Fig. 10. Far field for dilating profile.

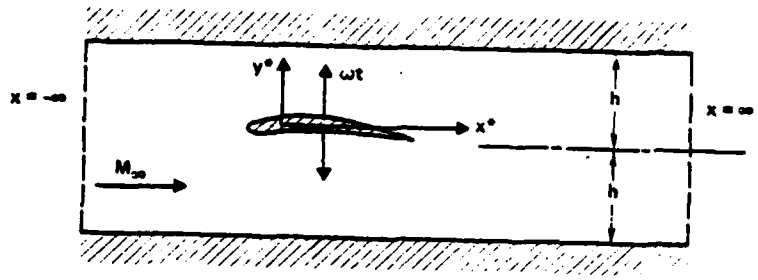

$$G = -\frac{2}{ih\sqrt{K}} \sum_{n=0}^{\infty} \frac{\varepsilon_n}{\omega_n} e^{-i\omega_n|x-\xi|} \left\{ \cos\frac{(2n+1)\pi y^*}{2h} \cos\frac{(2n+1)\pi\eta}{2h} - \sin\frac{(2n+1)\pi y^*}{2h} \sin\frac{(2n+1)\pi\eta}{2h} \right\}$$

$$\varepsilon_n = 2, \quad n > 0 \qquad \varepsilon_0 = 1 \qquad \omega_n \equiv \frac{\omega^2}{K^2} - \left[\frac{(2n+1)\pi}{2h}\right]^2$$

$$\Lambda = \frac{2}{ih\sqrt{K}} \sum_{n=0}^{\infty} \frac{\varepsilon_n}{\omega_n} \left\{ \cos\frac{(2n+1)\pi y^*}{2h} \cos\frac{(2n+1)\pi\eta}{2h} - \sin\frac{(2n+1)\pi y^*}{2h} \sin\frac{(2n+1)\pi\eta}{2h} \right\}$$

$$\times \int_{-1}^{1} f'(\xi) e^{i\omega_n|x-\xi|} d\xi \qquad \text{LINEAR}$$

$$+ \left[\int_{-\infty}^{\infty} \left\{ \cos\frac{(2n+1)\pi y^*}{2h} \cos\frac{(2n+1)\pi\eta}{2h} - \sin\frac{(2n+1)\pi y^*}{2h} \sin\frac{(2n+1)\pi\eta}{2h} \right\} d\eta \right]$$

$$\left[\int_{-\infty}^{\infty} Q(\xi,\eta,t) e^{i\omega_n|x-\xi|} d\xi \right], \quad \text{FOR } x^2 \to \infty \qquad \text{NONLINEAR}$$

N.B.: FOR $\omega \to 0$, NEED ONLY A FEW TERMS IN SUMS — OTHERWISE FAR FIELDS ARE PERIODIC AND LARGE.

Fig. 11. Dilating airfoil in presence of solid walls.

in FY 1979 are for harmonically dilating transonic airfoils between solid walls as well as in a free field. The structure obtained confirms the lack of damping of the disturbances for moderate frequencies as compared to the steady case. A similar result was obtained in FY 1978 using a heuristic model of a lifting airfoil as a pulsating vortex. Extensions of the systematic approximation procedure to treat lifting airfoils and wings using Kirchoff's formula and the present method are in progress.

Studies of Transonic Slender Body Flows

An inverse method is being applied to design slender bodies to support preassigned pressure distributions with the eventual application to cruise missiles and slender airplane shapes such as fighter configurations. In Fig. 12, results are shown for an axisymmetric solver which is being applied in the design mode. Special boundary discretization methods have been devised to provide consistency in the inverse mode. The excellent agreement with the experimental results of C8 attest to the accuracy of our procedures. Currently an iterative algorithm is being checked out for the inverse problem. An outline of the procedure is given in Fig. 13. Here, $R(x)$ is the body radius, g' is the nonlinear function related to the surface pressure coefficient, τ is the fineness ratio, and n is an iteration counter. The slender body theory employed for this phase has been generalized to provide indications of the existence of an unsteady equivalence rule which represents a new generalization of the steady theorem devised by Oswatitsch. Besides pointing to unconventional beneficial interfering concepts for reduction in wave drag, the results of this analysis could find application in cost effective means of calculation of dynamic longitudinal stability properties such as damping in pitch of slender vehicles and missiles in the transonic regime. An important cost savings will be achieved by the equivalence rule's removal of one of the spatial variables of the problem.

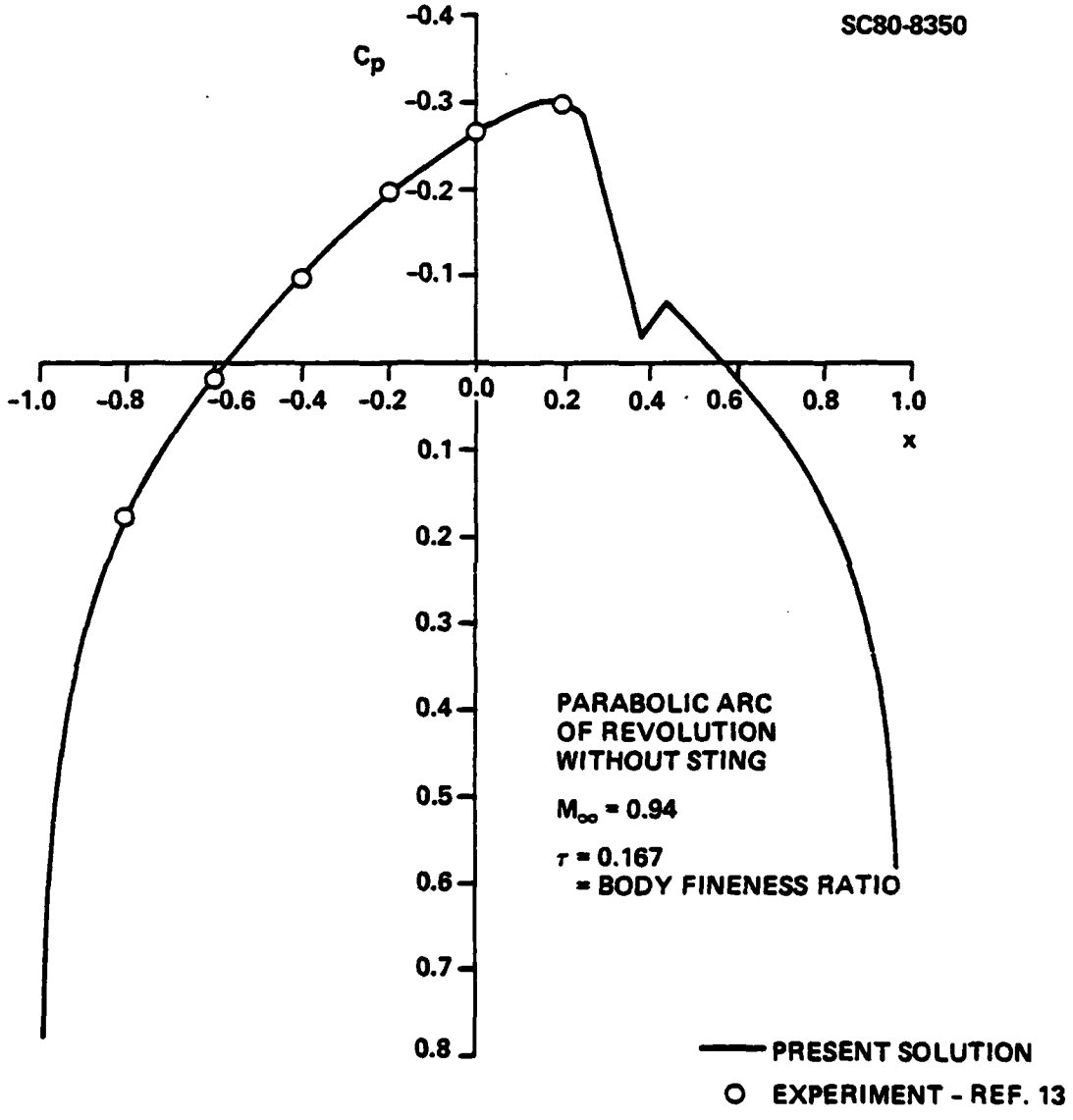

Fig. 12. Comparison with experiment of present slender body analysis code with design oriented boundary discretization. .

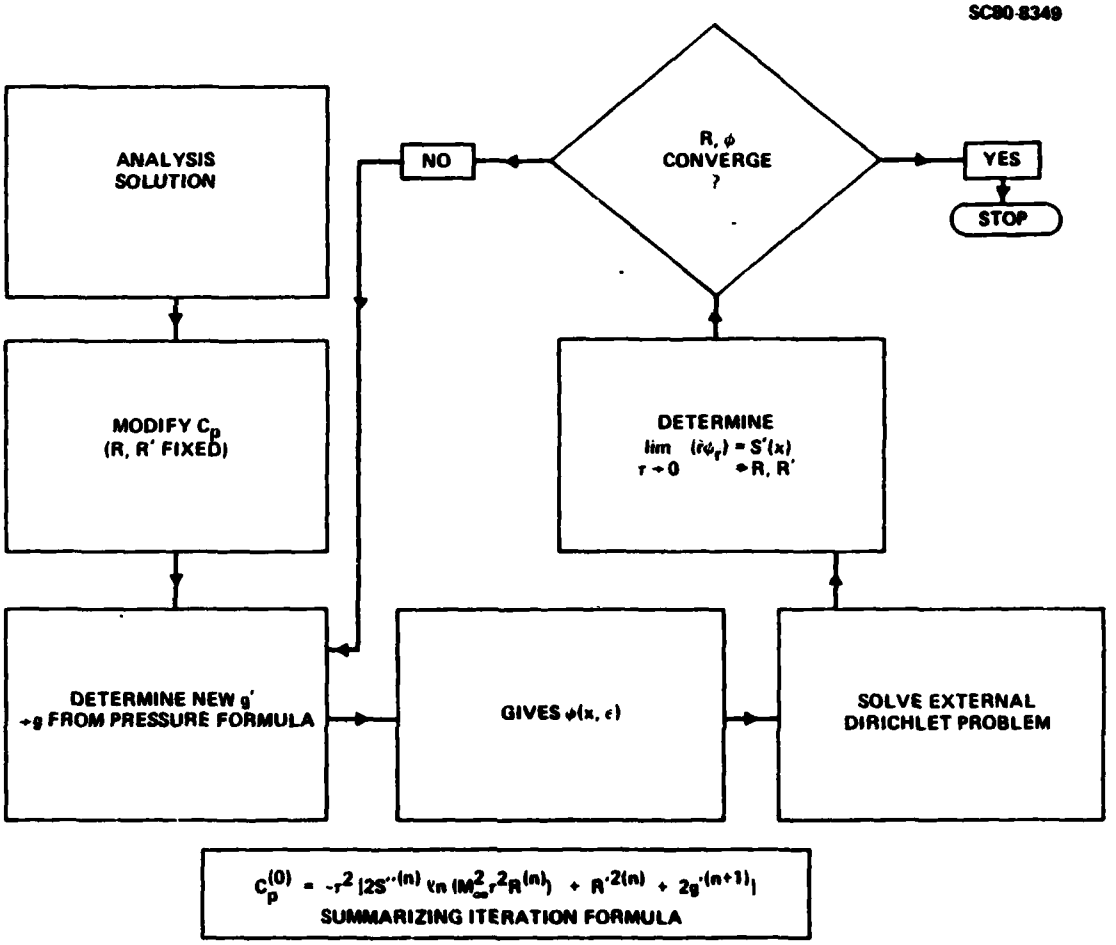

Fig. 13. Flow chart for slender body iteration procedure.

Cumulative Chronological List of Written Publications in Technical Journals

C1. Malmuth, N., "A New Area Rule for Hypersonic Wing Bodies," AIAA J. 9, December 1971, pp. 2460-2461.

C2. Malmuth, N., "Pressure Fields Over Hypersonic Wing Bodies at Moderate Incidence," J. of Fl. Mech., 59, Pt. 4, August 1973, pp. 673-691.

C3. Malmuth, N., "Generalized Area Rules and Integral Theorems for Hypersonic Wing-Bodies," AIAA J., 16, September 1978, pp. 1019-1022.

C4. V. Shankar, N.D. Malmuth, and J.D. Cole, "A Consistent Design Procedure for Transonic Airfoils and Wings in Free Field and Wind Tunnel," invited paper presented at NASA-Langley Conference on Advanced Airfoil Technology, March 7-9, 1978, in Proceedings.

C5. Shankar, V., Malmuth, N., and Cole, J.D., "Computational Transonic Airfoil Design in Free Air and a Wind Tunnel," AIAA Paper No. 78-103, January 1978, to be submitted with C6 to AIAA J.

C6. Shankar, V., Malmuth, N., and Cole, J.D., "Computational Transonic Design Procedure for Three-Dimensional Wings and Wing-Body Combinations," AIAA Paper 79-0344, presented at the 17th Aerospace Sciences Meeting, New Orleans, Louisiana, January 15-17, 1979, to be submitted to the AIAA J.

C7. Shankar, V., Malmuth, N., and Cole, J.D., "Transonic Flow Calculations Over Two-Dimensional Canard-Wing Systems," AIAA Paper 79-1565, presented at the AIAA 12th Fluid and Plasma Dynamics Meeting, July 23-25, 1979, Williamsburg, Virginia (expanded version in press for J. of Aircraft).

C8. Malmuth, N., "Wave Train Phenomena Over Hypersonic Wing Bodies," to be submitted to J. of Fl. Mech.

C9. Malmuth, N., Cole, J.D., Shankar, V., and Chakravarthy, S., "Asymptotic Far Fields of Wind Tunnel Flows," to be submitted to AIAA J.

C10. Cole, J.D. and Malmuth, N., "Non-Self Adjoint Boundary Value Problems in the Theory of Porous Wind Wall Interference," to be submitted to SIAM J.

INTERACTIONS

Papers Presented

I1. V. Shankar, N.D. Malmuth, and J.D. Cole, "Computational Transonic Airfoil Design in Free Air and a Wind Tunnel," AIAA Paper No. 78-103, January 1978, presented at AIAA 16th Aerospace Sciences Meeting, Huntsville, Alabama, January 16-18, 1978.

I2. N. Malmuth, "Current Nonlinear Problems in Aerospace," invited paper SIAM/ORA Meeting on Modern Applications of Mathematics, NASA-Dryden Flight Research Center, Edwards, California, November 17, 1977 (includes transonic and hypersonic results of this contract).

I3. N. Malmuth, "On a Class of Linear Hypersonic Flows," presented at Eighth U.S. Congress of Applied Mechanics, June 26-30, 1978, University of California at Los Angeles.

I4. V. Shankar and N.D. Malmuth, "Transonic Canard-Wing Interactions," presented at the Eighth U.S. Congress of Applied Mechanics, June 26-30, 1978, University of California at Los Angeles.

I5. Cole, J.D., "Contemporary Transonic Flow Problems," seminar presented at California Institute of Technology, February 9, 1979 (includes discussion of tunnel wall results on this contract).

I6. Malmuth, N., "Overview of Some Transonic Research Underway at Rockwell International Science Center," Unsteady Transonic Aerodynamics Workshop, sponsored by AFFDL, Ohio State University, November 17, 1978.

I7. Malmuth, N., "Transonic Flow in Adaptive and Nonadaptive Tunnels," presented at AEDC Working Session on Adaptive Wall Research, February 26, 1980.

Consultative and Advisory Functions to Laboratories

Dr. Malmuth has been a member of the NASA Ad Hoc Committee on Space Shuttle Orbiter Hypersonic Aerodynamics and is presently a member of the Industrial Steering Committee for the NASA-Ames National

Aerodynamics Simulation Facility. This committee has Dr. W.F. Ballhaus as its chairman and meets approximately twice yearly. Other individuals on this committee include P. Rubbert, R. Melnik, W. Hankey, and F.R. Bailey.

Other Interactions

Dr. Malmuth is chairman of the Rockwell fluid dynamics technical panel and serves on the AIAA Fluid Dynamics Committee.

Other Statements

The thrust of the research effort is to couple asymptotic methods with computational techniques to enhance the efficiency of the latter in analyzing nonlinear flows. Results obtained from the far field activity and application of new nonlinear slender body design methods to be developed in the next phase of this contract should provide the basis of handling three-dimensional configurations to achieve marked reductions in the cost of transonic aerodynamic design and analysis. In this regard, the consistent inverse design procedure developed under Rockwell IR&D and reported in C4 and C6 will be applied in this effort to achieve optimum configurations. An immediate fallout of this effort should be applications to cruise missile design. Other derivatives of the work will be the development of technology baselines for the design of the next generation of energy efficient and high performance tactical and strategic vehicles.

List of Professional Personnel Associated with Research Effort

N. Malmuth, J.D. Cole, V. Shankar, D. Anderson, and S. Chakravarthy.